Modelling the Ruin of Forests under Climate Hazards

Pascal Yiou[1] and Nicolas Viovy[1]

[1]Laboratoire des Sciences du Climat et de l'Environnement, UMR 8212 CEA-CNRS-UVSQ, IPSL & U Paris-Saclay, 91191 Gif-sur-Yvette Cedex, France

Correspondence: P. Yiou (pascal.yiou@lsce.ipsl.fr)

Abstract. Estimating the risk of collapse of forests due to extreme climate events is one of the challenges of adaptation to climate change. We adapt a concept from ruin theory, which is widespread in econometrics or the insurance industry, to design a growth/ruin model for trees, under climate hazards that can jeopardize their growth. This model is an elaboration of a classical Cramer-Lundberg ruin model that is used in the insurance industry. The model accounts for the interactions between physiological parameters of trees and the occurrence of climate hazards. The physiological parameters describe interannual growth rates and how trees react to hazards. The hazard parameters describe the probability distributions of occurrence and intensity of climate events. We focus on a drought/heatwave hazard. The goal of the paper is to determine the dependence of ruin and average growth probability distributions as a function of physiological and hazard parameters. From extensive Monte Carlo experiments, we show the existence of a threshold on the frequency of hazards beyond which forest ruin becomes certain in a centennial horizon. We also detect a small effect of strategies to cope with hazards. This paper is a proof-of-concept to quantify collapse (of forests) under climate change.

1 Introduction

~~If one adopts the (debatable) dogma that ecosystems provide services to society, one must also accept that such services could disappear under natural or human made hazards. In many instances, such ecosystems are considered as "investments" that "investors" want to fructify some time later. A challenge is to estimate the risks associated to such investments.~~ Extreme events such as droughts and heatwaves are climate hazards that have short and long term effects on forests. The recent accumulation of drought/heat stress to forests might lower their resilience to future extreme events (e.g. Wigneron et al., 2020; Flach et al., 2018; Bastos et a . It has been observed that such events increase the chance of tree mortality (Anderegg et al., 2013). Such an effect questions the survival of tree species in some regions of the world (Zeppel et al., 2011; Lindenmayer et al., 2016). The mechanisms leading to tree mortality include complex physiological processes that can depend on the tree species and type of hazards (e.g. Choat et al., 2012).

Most studies on tree death are based on direct or indirect observations of the tree behavior and their growth parameters. They give precious information on the observed global response of forests to those climate hazards. But they are by essence

limited to the length of the observation period, and have mostly focused on a few key observed events (e.g. Rao et al., 2019) , which can hinder a statistical description that would be necessary to build projections, or estimate *risk* (Field et al., 2012) as a response to climate change. Here *risk* is understood as the probability distribution of a failure (e.g. irreversible damage or death) due to climate hazards (Katz, 2016).

The potential disappearance of whole forest or a given tree species, due to changes in climate features can be qualified as a *tipping point* of climate change. There has been ample literature on ~~*tipping points*~~ tipping points of the climate system, i.e. climate thresholds beyond which ecosystems change behavior ~~(Lenton et al., 2008; Levermann et al., 2012). Most of those papers are rather qualitative in that they do not give probabilities of "tipping point" nor provide a timing for such changes. A consequence is that policymakers make little use of those studies, because risks are rarely estimated in precise ways.~~ (Lenton et al., 2008; Levermann et al., 2012, just to cite seminal papers). Those papers have defined methodologies to identify climate thresholds beyond which ecosystems are endangered. They have been used to infer tipping points of forests (Reyer et al., 2015; Pereira and Viola, 2018).

~~A body of literature on so-called *collapsology* has emerged in the past few years (Diamond, 2005). Those studies describe mechanisms that would make the key institutions of society collapse due to an accumulation of big or small events. Again, those considerations are generally qualitative as to "when" and "how intense", as they address very general issues and no mechanistic model of a collapsing system is analyzed.~~

~~Most of those studies are useful to raise awareness on the dangers of climate change, but are rarely included in decision chains. On the other hand, there~~ The key concept of this paper is the use of the so-called *ruin theory* to provide quantitative elements on the probability of such tipping points. There have been many papers in the econometrics literature that describe ruin models for insurance and finance since the seminal work of Lundberg (1903). A mathematical and statistical artillery (Asmussen and Albrecher, 2010) has helped determining the optimal parameters of such models, so that insurers or investors limit the risk of losing their investment and maximize their gain. Ruin models are used to describe the probability that a company that grows with regular income can get bankrupt due to external hazards. To the best of our knowledge, this literature has never been transposed to environmental sciences~~, although it provides all the tools for decision making, which are used daily in insurance and finance.~~ .

~~The goal of~~ The rationale of the choice of trees or forests in this paper is ~~to obtain quantitative parameters thatdescribe the ruin of ecosystems. We chose to focus on forestry, for which mechanistic growth models~~ that, as opposed to annual plants, trees are adapted to live for a long time and then should be able to survive to bad climate conditions on a given year. Mechanistic growth models for trees can be devised (e.g. Han and Singh, 2020) and observations of tree mortality are available (e.g. Choat et al., 2012). Tree growth is affected by climate variations in various ways. Heatwaves and droughts can alter (and lower) tree reserves and the capability for growth ~~on next years~~ during the years following a climate event, which affects their average growth and can increase their chance of mortality (von Buttlar et al., 2017; Sippel et al., 2018). ~~The recent accumulation of drought/heat stress to forests might lower their resilience to future extreme events (e.g. Wigneron et al., 2020; Flach et al., 2018; Bastos et al., 2020) . Several studies have investigated the processes leading to tree mortality from observations (Adams et al., 2009; Bigler et al., 2007; Bréda a~~

A parallel between insurance system and trees can be done. As opposed to annual plants, trees are adapted to live for a long time and then should be able to avoid death related to damage due to bad climate conditions during a year. Those damages can be related to a reduced productivity and in the worst cases to a destruction of a part of the trees (related for instance to xylem embolism that kills the branches). For this purpose, they contain a large amount of carbohydrate and a structure (branches)that non structural carbohydrates (NSC). These NSC reserves allow to build rapidly a large surface of leaves (potential productivity been is related to this foliage area)) on during the next yearand protect from pathogen disease even if the productivity of the previous year was reduced or because of events like defoliation (e.g insects); they help renewing the leaves in case of defoliation (related to frost or insects, for instance) and, more generally, provide the necessary energy for metabolism, including protection from pathogen diseases. Hence a part of annual productivity is devoted to accumulate carbohydrate reserves (i.e., larger than what is necessary for the next year initiation of the vegetative cycle)and ensure a structure that allows to support leaves. This can . As there is a competition in allocation of assimilates between NSC and plant growth, the plant does not accumulate reserves indefinitely, but tends to reach an optimum value (Barbaroux et al., 2003). Climate hazards can reduce the quantity of assimilate allocated the NSC (He et al., 2020). This can be caused directly by reducing productivity. But it can also indirectly cause a plant damage like xylem embolism. This embolism can kill trees in extreme cases (especially for young trees). But this process kills only parts of mature trees, which affects the total amount of NSC, but also affects the surface to develop a new foliage and jeopardizes the ability to grow during the following years. So even though this effect does not directly impact NCS reserves, it induces equivalent consequences for tree growth in years following climate hazards. Several studies have investigated the physiological processes leading to tree mortality from observations (Adams et al., 2009; Bigler et al., 2007; Bréda and Badeau, 2008; Villalba and Veblen, 1998; Matusick et al., 2018). These studies compare relative tree ring growth between death and healthy surrounding trees with same diameter during the years prior to tree death. This comparison, by removing annual climate effects, is then a good proxy of the difference in NSC reserves. These studies conclude that dying trees have a systematic level of reserves lower than for living trees. Hence, even if trees are not fully depleted of NSC, there is a critical level of NSC under which trees cannot recover and then die. Then these studies conclude that measurements of the level of NSC in trees are good indicators of possible forest die-back. NSC can hence be compared to an insurance system when each year, a part of the productivity is "payed" to the insurance (i.ecarbohydrate reserves. NSC for trees) but in return can be mobilized in case of damage. Then "ruin" occurs when trees die because of carbon starvation as level of carbohydrate reserves and productivity is not sufficient to maintain respiration costthe level of NSC reach a critical level under which the probability of tree death on the short term become very likely. This loosely justifies a parallel between insurance and tree systems.

At present, full size mechanistic models of tree growth forced by large ensembles of climate simulations (e.g. Massey et al., 2015) require a computing power that limits the volume of numerical experiments that can be performed to estimate reliably probability distributions. This is why we opted to devise a simplified model, from the Cramer-Lundberg toy model.

The goal of this paper is to formulate a simplified model of tree growth and the impacts of climate hazards, which can be interpreted as a ruin model, and make ensemble simulations of that model in order to evaluate its sensitivity to hazard parameters.

~~Our~~ Hence our study investigates the probability of "ruin" of a population of trees that are subjected to heat and drought stress. ~~We introduce a~~ In this context, (tree) ruin is reached when the carbon reserve goes under a critical threshold that no longer guarantees the growth of trees. This concept of ruin can be applied to a forest in general, but also to a given tree species, which means that this species will disappear from the forest but that a forest with other more tolerant species can still survive.

Section 2 introduces a growth/ruin model for trees based on a Cramer-Lundberg ruin model, and discuss the interpretation of its parameters (section 2.1). Section 2.2 introduces a simple tree growth model based on the Cramer-Lundberg ruin model for insurances (Embrechts et al., 1997). We investigate its properties in order to evaluate the occurrence of ruin (i.e. ~~disappearance of trees~~ when trees stop growing) within a fixed horizon, due to the impacts of extreme events, under various climate ~~change scenarios.~~ scenarios. Here, the term "horizon" is the maximum (finite) period for which simulations are made, which in practise, can be viewed as the end of the 21st century. This approach is meant to tackle quantitatively the issues of tipping points ~~or collapse~~ of ruin for a specific field (forestry), although this could be extended to other domains. By *quantitative*, we mean that we determine the probability distributions of key ruin parameters (e.g., time of ruin and average ~~capital~~carbon reserve). Unlike the Cramer-Lundberg ruin model, our tree model cannot be solved explicitly and we will resort to extensive numerical simulations, as a standard sample for the insurance industry has to contain more than 10^4 members for proper probability estimates.

~~In section 2 we introduce a growth/ruin model for trees based on a Cramer-Lundberg ruin model, and discuss the interpretation of its parameters. In section~~ In section 3 we detail the meteorological data that are used to construct a ~~hazard function~~ damage function (due to climate hazards). Section 4 explains the experimental protocol for the analyses. The results and interpretations are developed in section 5. An Appendix is devoted to the development of a drought index based on precipitation and temperature.

2 Methods

2.1 Cramer-Lundberg ruin model

This section introduces the key concepts ~~to~~ of ruin models. The insurance industry uses such statistical models to determine the premium ~~prices,~~ rates in order to ~~achieve a balance between competing companies and minimize the risk of ruin (i.e. when the capital vanishes) .~~ avoid ruin (here: bankruptcy) when hazards occur. Those statistical models are based on the simple Cramer-Lundberg model (Asmussen and Albrecher, 2010; Embrechts et al., 1997), which can be formulated as:

$$R(t) = R_0 + p{\cdot}t - S(t), \tag{1}$$

where $R(t)$ is the insurance capital at time t, $R_0 > 0$ is the initial capital, $p > 0$ is the premium rate that is collected every year t, and $S(t) \geq 0$ is a damage function that represents the (random) losses to hazards that occur up to time t. The only random part of the model in Eq. (1) stems from the ~~loss~~ damage function $S(t)$. A ruin is declared and the process is stopped when $R(t) \leq 0$. If $S(t)$ is always 0, then the capital grows indefinitely. The literature on ruin theory describes how the probability distribution of $R(t)$ depends on hypotheses on hazards conveyed by the random damage function $S(t)$.

One can be interested in the behavior of the system before a finite horizon $T > 0$, e.g. a few decades. We define the ruin probability Ψ before horizon T by:

$$\Psi(R_0, p, T) = \Pr\left(R(t) \leq 0, \text{ for some } T \geq t > 0\right) \tag{2}$$

and the ruin time $\tau(R_0, p, T)$ by the first positive time when ruin is reached:

$$\tau(R_0, p, T) = \inf\{t > 0, R(t) \leq 0\}, \tag{3}$$

where $\inf A$ is the infimum value of the set A. Since $S(t)$ is a random ~~process~~variable, we are interested in $E(\tau)$, the expected value of τ with respect to the random variable $S(t)$. If ruin never occurs during simulations of R, then $E(\tau) = \infty$. Actors in insurance companies try to estimate the smallest ~~p rate~~ premium rate p from expert knowledge on the probability distribution of $S(t)$ in order to avoid ruin, ~~which would~~ as it is assumed that the lowest p would make them more attractive to clients, and hence would give them a lead in the competition against more greedy companies (which are subject to the same ~~hazards~~ damages $S(t)$).

In several instances, there is no acceptable value for p to prevent from ruin, i.e. the probability distribution of the expected value of τ can be lower than the value T (say, with some low probability). This is why insurance companies resort to re-insurance to avoid bankruptcy after unexpectedly large losses $S(t)$.

The ~~losses~~ damages $S(t)$ are generally represented as a *random sum* of random variables:

$$S(t) = \sum_{k=1}^{N(t)} X_k, \tag{4}$$

where $N(t)$ is a Poisson random variable that accounts for the number of hazards occurring up to time t, and X_k are random variables that account for the cost of each hazard. A Poisson distribution is meant to express the number of events that occur in a fixed period of time. Hence, the probability distribution of $N(t)$ can be written:

$$\Pr(N(t) = n) = \frac{\lambda^n}{n!} e^{-\lambda}, \tag{5}$$

where $\lambda > 0$ is called the intensity of the Poisson distribution. The mean and variance of the Poisson distribution are λ.

The probability distribution of X_k can be modeled by an extreme value law, like a generalized Pareto distribution (GPD) (Coles, 2001; Embrechts et al., 1997), when a hazard variable exceeds a high threshold u. The GPD describes the probability distribution of a random variable X when its value exceeds a threshold u:

$$\Pr\{X > x | X > u\} = \left[1 + \xi\left(\frac{x - \mu}{\sigma}\right)\right]^{-1/\xi}, \tag{6}$$

where $\sigma > 0$ is a scale parameter and ξ is a shape parameter that states how fast extremes grow. The parameters of the Poisson distribution for $N(t)$ and the GPD distribution are estimated from prior information, e.g. observations or expert knowledge.

There is ample statistical literature in finance on the relation between τ and the probability distribution of S (Embrechts et al., 1997; Asmussen and Albrecher, 2010). In practice, estimates of $E(\tau)$ or an optimal p can be obtained by simulating the model of Eq. (1) and estimating empirical probability distributions.

The notion of finite horizon T is useful when considering that an investment (in the insurance sector) is made for a finite time. We will be interested in generating many finite sequences of $S(t)$, corresponding to a sample of all possible T-long trajectories.

2.2 A ruin model for trees

The goal of this sub-section is to adapt the Cramer-Lundberg model in Eq. (1) to formulate a simple tree growth model that explicitly takes into account a ~~climate hazard~~ damage $S(t)$ due to a climate hazard, such as drought and heatwave.

Here $R(t)$ is the non-structural carbohydrates (hereafter called reserves) that allow tree growth at the beginning of the vegetative period. We assume that trees spend a fraction of their ~~resources to grow roots and leaves~~reserves to grow their different plant organs (e.g. roots, stem, leaves...), depending on their previous state. ~~We~~ As stated previously, we also assume that tree resources are bounded by a maximal value $R_{\max}$ (Barbaroux et al., 2003). The value of $R_{\max}$ sets the scaling of the reserve $R(t)$. In the rest of the paper, the reserve will be expressed in percentage of $R_{\max}$, with values between 0 and 100 %. ~~Indeed labile carbon does not grow indefinitely. When a sufficient level of carbohydrates is reached, allocation preferentially goes to the growth of the different organs. This justifies the use of an upper limit for R.~~

There have been observations of legacy effects of drought hazard on the tree growth during the year after the drought (Anderegg et al., 2015b). This effect depends on the tree species. Because of this decreased ~~NPP~~net primary production (NPP), we assume that it also affects the allocation to carbohydrate reserves. Hence, the yearly NPP allocated to reserves $p(t)$ depends on the climate hazard damage that occurred during the previous year $S(t-1)$:

$$p(t) = p_0 - BS(t-1), \tag{7}$$

where p_0 is the optimum average yearly net primary production (NPP) of a population of trees allocated to reserve, and $B \geq 0$ is a memory factor of the damage function. More generally, p_0 represents the fraction of NPP allocated to R when NPP is itself optimum. But it has been observed from in-situ measurements that the total NPP decreases the year after a hazard (Anderegg et al., 2015b). In general, this is related to the fact that plants have lower leaf area and/or and increased respiration cost related the investment to repairing tissues or defensive costs. So Eq. (7) does not represent a change in the fraction of total NPP allocated to reserve, but the fact that the total amount of carbohydrate allocated to reserves decreases because of the decrease of total NPP, assuming that the fraction allocated to R is unchanged. In principle, the value of p_0 can depend on the tree species or location.

We hence introduce a new growth/ruin model for trees that describes the carbon reserve R variations with time:

$$R(t) = \min\left[(1-b)R(t-1) + p(t) - S(t), R_{\max}\right], \tag{8}$$

where $b \geq 0$ is the fraction of previous resources (at time $t-1$) devoted to growth. For a steady state system, b is equal to p_0 In this model, the parameters b, B and $R_{\max}$ are called *physiological* as they describe tree growth. We define *tree ruin* when $R = 0$, (i.e. NSC reach a critical low level where tree death become almost certain.

In this paper, we suppose that the type of hazards that can affect tree growth (or survival) are summer droughts (Allen et al., 2010; Choat et al., 2012; DeSoto et al., 2020). In Europe, major summer heatwaves are often concomitant with droughts.

This combination of climate factors creates a stress to trees, which lowers their NPP and can destroy branches and leaves and impacts their growth and reserve. Other types of hazards could also be considered (storms, pests, etc.). ~~We declare that ruin is reached when $R(t) = 0$.~~

The hazards do not necessarily occur every year: they arrive at times t that ~~follow~~ can be modeled by an exponential distribution with parameter Λ (Coles, 2001). Thus the inter-arrival times follow a Poisson distribution with a mean value of $\theta = 1/\Lambda$ (the average return time of hazards). This description is rather generic ~~in standard queuing models (Feller, 1950)~~has been widely used in atmospheric sciences or statistical climatology (e.g. von Storch and Zwiers, 2001; Smith and Shively, 1995). When climate hazards occur (at random times), the corresponding damage $S(t)$ is written as:

$$S(t) = A_h \sum_{k=1}^{N(t)} X_k. \tag{9}$$

A_h is a normalizing constant that translates the climate hazard conveyed by X_k into damage to $R(t)$. $N(t)$ is the number of hazards (e.g. the number of very hot/dry days) during year t and follows a Poisson distribution with parameter λ. X_k are climate variables like a drought index for heatwaves or wind speed for storms during hazards, and follow generalized Pareto distributions (GPD), with scale parameter σ and shape parameter ξ. The GPD describes the probability distribution of X_k when it exceeds a high threshold u (Coles, 2001). The parameter of the GPD (σ and ξ) and the occurrence of events (λ and Λ) are called the *hazard* parameters.

When no hazard occurs, $S(t) = 0$. If $b = 0$ (no use of reserves for growth), $B = 0$ (no memory of previous hazard) and $N(t) = 1$ (only one hazard at a time at most), then the model in Eq. (8) simplifies to the Cramer-Lundberg ruin model (Eq. (1)), in which $N(t)$ follows a Poisson distribution of parameter Λ. If hazards never occur (i.e. $S = 0$ at all times), then $R(t)$ converges to $(1 - b)R_{\max}$.

The parameters of the Poisson distributions for $N(t)$ and the Pareto distributions for X_k can be estimated experimentally from meteorological observations or climate model simulations. The growth parameters p, b and $R_{\max}$ in Eq. (8) can be obtained from tree physiology databases (Allen et al., 2010; Cailleret et al., 2017) and should be adapted to tree species.

The difficult part is to estimate scales for the values of A_h and B. It has been observed that tree species can have differing strategies to face heat and drought stress (Adams et al., 2009; Teuling et al., 2010): some tree species grow in spite of the hazard during year t. ~~this~~ This can be achieved by maintaining stomatal aperture to maintain photosynthesis (anisohydric strategy) increasing the risk of embolism (Mitchell et al., 2013) or changing allocation to maintain growth of branches and root at expense of carbohydrate reserves (van der Molen et al., 2011). In both cases, these trees "pay" the next year, even if there is no hazard because maintaining the plant growth ~~will be~~ occurs at expense of foliage surface and plant protection on next year (van der Molen et al., 2011). Those are trees with interannual memory. Conversely other tree species stop growing during hazards (by stomatal closure to avoid embolism (isohydric strategy) or maintain allocation to reserve at the expense of other pools) at t~~,~~. For these trees, the impact on growth on the year of hazard is important, but this hazard has few impacts on the next year. Those are trees without interannual memory. Even if the two strategies are more general strategies than anisohydric/isohydric (as it also includes possible change in allocation to growth/reserve), in the following we will use the terms anisohydric/isohydric as it is widely used to describe different responses to drought. It is possible to represent the different strategies in the model through

the parameter B. Hence the ~~first~~ anisohydric strategy (i.e. maintaining growth, interannual memory) can be represented by ~~high~~ positive value of B in Eq. (7). Conversely the ~~second~~ isohydric strategy (i.e. conservative, no memory) can be represented by B close to 0 in Eq. (7). We will investigate the sensitivity of the ruin probabilities to those tree strategies. Therefore, to simplify ~~things, making~~ the terminology, we make a parallel with an insurance system: if $B = 0$, trees pay "cash" on their reserve ($S(t)$ then ~~will be large~~ is large when hazard occurs); if $B > 0$ ~~they~~ trees allow for a "credit" to the next year ($S(t)$ is reduced but ~~will impact~~ impacts the possibility to use reserve on next year). Mitchell et al. (2013) notice that ~~in reality,~~ there is a continuum between the two strategies which can be represented by the value given by B. The values of B are chosen so that the average value of damages (i.e., the expected value of $(1 + B)S(t)$) is a constant. This constant gives the scale of the impact parameter A_h.

In this paper, the values of A_h and B are arbitrarily chosen to scale with an expected behavior of trees. The range of those parameters could be estimated from in situ observations or expert knowledge. In this proof-of-concept paper, those parameters are considered to be normalized and do not have units.

2.3 Sample trajectories

~~The time variations of this model are illustrated with parameters of tree growth $p = 5$, $b = 0.05$, $A_h = 0.6$, $R_{\max} = 100$.~~ For simplicity, we normalize all the parameters to the optimum level of reserve $R(t)$ fixed the an arbitrary value of 100. So $R_{\max} = 100$. likewise $R(t) = 0$ which is the value for tree ruin, as explain in introduction, do not necessarily means a totally depleted NSC reserve but a level for which the probability of tree recovery becomes very unlikely even for good weather condition, and trees will die in the short term. (Barbaroux et al., 2003) evaluated the seasonal evolution of NSC for beech trees. The amount of NSC in July (which correspond to the minimum of the NSC cycle) reaches 75% of its maximum. Hence we assume that annual allocation and use of the NSC is 25% of the total (i.e. $p_0 = 25$ and $b = 0.25$). Likewise He et al. (2020) evaluated the impact of several level of droughts on total NSC. They estimate a decrease of NSC of 20% in case of large drought. Then we took $A_h = 1.2$ so that damages scale to ≈ 20. The hazard parameters are $\sigma = 0.1$, $\xi = -0.2$ and threshold $u = 1$ (from the GPD distribution of a drought index), and $\lambda = 10$ days and $\Lambda = 5$ years for the hazard arrivals. The model was run with memory parameter values of $B = 0$ (isohydric or "cash") and ~~$B = 1.5$ (~~$B = 0.4$ (anisohydric or "credit"). We simulated 10^4 trajectories with those parameters. For each ensemble, we computed the average of the reserve function $R(t)$ before it reaches $R(t) = 0$. We selected four trajectories with the 95th, median and 5th quantiles of the average reserve function, and one of the trajectories with a ruin ~~.~~(i.e. ruin time is $\tau < 100$).

Figure 1ab shows the time series of the damage $S(t)$ and the reserve $R(t)$ functions for those four key trajectories, when $B = 0$ (~~"cash"~~isohydric). As the shape parameter ξ is negative, the damage values $S(t)$ do not yield a large variability ~~. The~~ (i.e., unbounded). The statistical properties of all trajectories of $S(t)$ are supposed to be similar, as they are drawn from the same probabilistic laws. Therefore, we chose to show only two trajectories for $S(t)$: one that achieves ruin (in red) and the one with the median value of the $R(t)$ mean. In this experiment, the reserve averages for the 5th, median and 95th ~~and median~~ quantile trajectories are respectively ~~42, 69 and 72~~ 74, 84 and 88 reserve units.

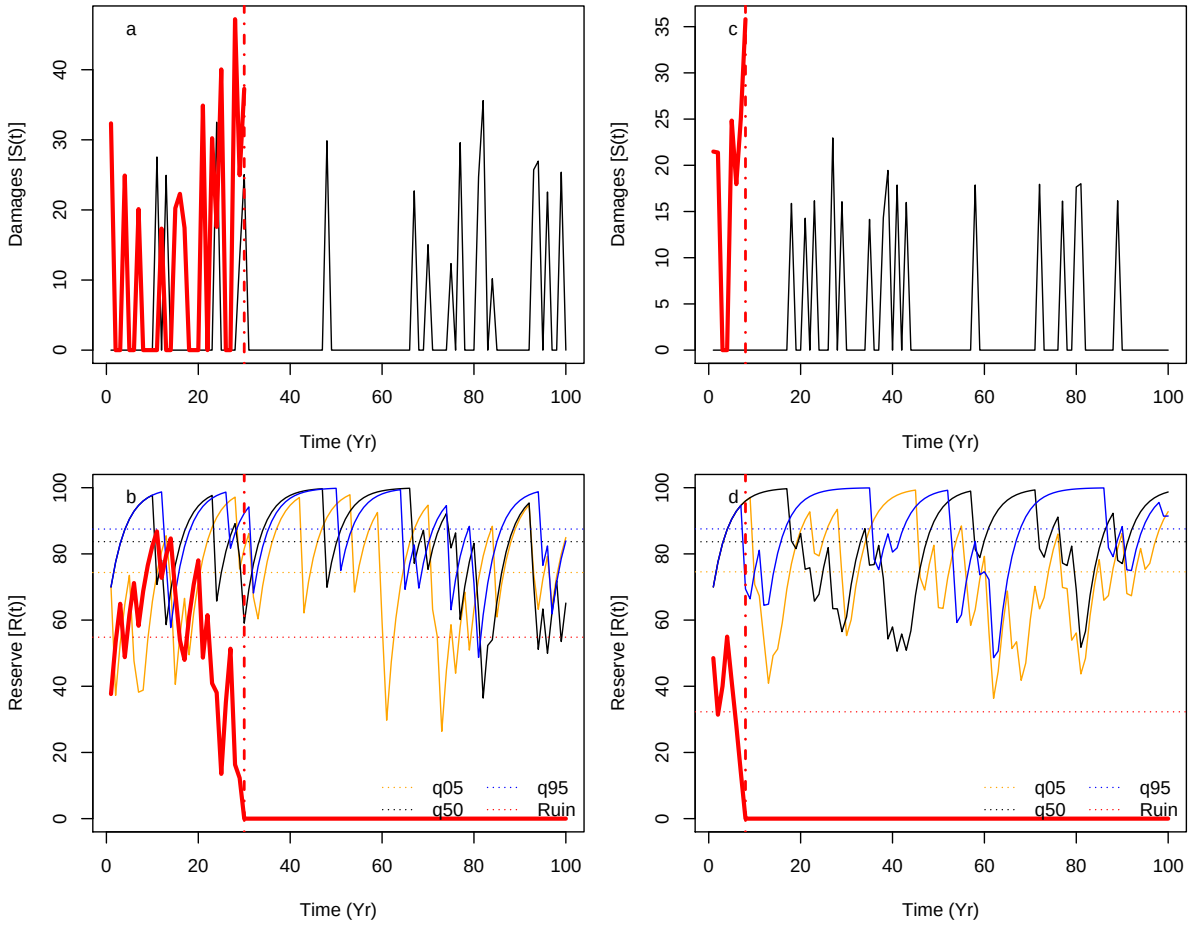

Figure 1. Sample of ~~four~~ time series of simulations of $S(t)$ (upper panels) and $R(t)$ (lower panels) for $B = 0$ (~~"cash"~~isohydric: panels a and b) and ~~$B = 1.5$~~ $B = 0.4$ (~~"credit"~~anisohydric: panels c and d). The ~~blue~~ red lines ~~are the~~ show sample trajectories of ~~S~~ $S(t)$ and ~~R that achieves~~ $R(t)$ for which $R(t)$ reaches 0 for $t < 100$. A vertical dashed-dotted line indicates the ~~median~~ time of ~~the average of R (among 10^4 simulations)~~ruin. The black lines ~~are~~ indicate trajectories of $S(t)$ and $R(t)$ (for $B = 0$ and $B = 0.4$) that achieve the ~~trajectories~~ median of the ~~95th quantile~~ mean of ~~R~~all 10^4 trajectories of $R(t)$. The orange and blue lines ~~are for~~ in panels b and c show the ~~5th quantile~~ trajectories of ~~R~~$R(t)$ that achieve the 5th and 95th quantiles of all 10^4 simulation means. The ~~red lines is for trajectories with ruin. The~~ horizontal ~~dotted~~ dashed lines ~~indicate~~ of the ~~mean $R(t)$ values~~ lower panels (b and c) represent the means of the ~~selected~~ represented trajectories, for times before ruin.

Figure 1c,d shows the time series of the damage $S(t)$ and the reserve $R(t)$ functions for four key trajectories, when ~~$B = 1.5$ ("credit"~~ $B = 0.4$ (anisohydric). The damage function yields the same statistical properties but the scaling is different so that the integrated damages are similar in both cases: the hazard is scaled so that the damage at year t is distributed over t and
260 $t + 1$. On this sample of simulations, the reserve averages for the 5th, median and 95th quantiles ~~and median~~ trajectories are

respectively ~~42, 69 and 72~~ 75, 84 and 88 reserve units. Hence, the reserve ~~is very similar , although the ruin time could occur later. The time variability of~~ average values seem very similar in both experiments. The reserve $R(t)$ ~~is smoother as $B = 1.5$ introduces an interannual memory of hazards. This explains the long-time variability of the median trajectory, compared to Figure 1ab.~~

~~Those two samples of parameters illustrate that the coping strategies do influence the behavior of the modeled trees. Ruin can occur faster~~ with $B = 0.4$ yield a slightly slower variability for the upper values (black and blue lines in Fig. 1b,d), which is explained by the memory induced by $B > 0$. The empirical probability of reaching a ruin within 100 years (see Eq. (2)) is higher for $B = 0$ (~~paying "cash") , although the median of the reserve is higher. The rest of the paper is devoted to quantify those differences.~~ $\Psi = 4 \cdot 10^{-3}$) than for $B = 0.4$ ($\Psi = 1.5 \cdot 10^{-3}$). In both cases, ruin is a rare event for those physiological parameters, and the return period of a ruin (i.e. the inverse of its probability) is larger than 100 years. This justifies our statistical approach of simulating a very large ensemble of trajectories, as the key difference between tree strategies lies on small probability that is difficult to assess from observations.

~~A~~

A physical evaluation of the model is in principle difficult. The main reason stems from the nature of the phenomenon that is modeled, which does not occur very often. The ruin of insurance companies hardly ever occurs for a complete validation of the Cramer-Lundberg model, and this could be a heuristic argument that it works (at least for that domain of application). In practice, a lot of data have been collected from ~~death~~ dead trees and from surrounding trees still alive to evaluate how ~~death~~ dead trees behave years before they die (e.g. Villalba et al. (1998), Bréda and Badeau (2008)). Hence ~~difference~~ differences of tree rings width between dead and living ~~tree~~ trees (that allow to remove the influence of annual climate condition) can be considered as a good proxy of tree reserves. Cailleret et al. (2017), ~~for instance~~ made a synthesis of ~~existing data and investigated tree ring growth years before tree death~~these data on differential tree growth used as proxy of NSC, under various climate hazards. ~~It is interesting to notice that there is~~ There is a good agreement between our simulated evolution of reserves in case of ruin (Figure 1b,d) and observed evolution of ~~tree ring width before tree dying~~relative tree ring growth before tree death. In particular Cailleret et al. (2017) show that in ~~the majority of the~~ a majority of cases, there is an observed relative decrease of growth ~~(compared to healthy trees)~~ between twenty to fifty years before death, which is coherent with our simulations. A thorough physical verification would be a whole project in itself, so that this paper focuses on the analysis of the behavior of the tree ruin model.

3 Data

The goal of this section is to provide climate constraints on the parameters of the hazard function $S(t)$.

3.1 Observations

Meteorological data were taken from the European Climate and Data (ECA&D) database (Haylock et al., 2008). We used daily maximum temperature (TX) and daily precipitation (RR) from Berlin, De Bilt, Orly, Toulouse and Madrid stations. This

Table 1. ~~Distribution~~ Range of ~~scale~~ values of parameters for the damage function $S(t)$ from the I_{YV} drought/heatwave (~~upper panel~~HW) index computed for the five stations. The GPD thresholds are the averages of the 95th quantiles of the index for the five stations. The GPD scale and shape ~~(lower panel)~~ parameters are the averages of the ~~I_{YV} indice~~ estimates on the indexes for ~~Berlin, De Bilt, Orly, Toulouse and Madrid~~each of the five stations. The ~~vertical bars represent the 95% confidence intervals~~ ranges of the ~~estimates~~GPD parameters take the uncertainties into account.

Parameter	Interpretation	Average value	range
u	GPD threshold	1.7	$[1;5]$
σ	GPD Scale	0.15	$[0.08;0.2]$
ξ	GPD shape	-0.32	$[-0.45;-0.2]$
λ	Nb. dry days	15	$[2;30]$
Λ	Return period of HW events (years)	8	$[2;15]$

choice was motivated to cover a rather large range of European latitudes and longitudes over western Europe. We considered data from 1948 to 2019 ($>$ 70 years of daily data). Those datasets yield less than 10% of missing observations.

3.2 Drought/heatwave damage index

We consider the drought/heatwave index I_{YV} defined in the Appendix A, based on precipitation frequency and temperature from the ECA&D database. This index is computed over five ECA&D stations (Berlin, De Bilt, Orly, Toulouse and Madrid). Quite a few drought indexes already exist. On the one hand, the most relevant ones are based on soil moisture, but they do not cover a period that it long enough to determine the GPD parameters of its extremes. On the other hand, indexes that use well measured meteorological variables (e.g. temperature and precipitation) are not fully adapted to reflect drought (see Appendix A). Therefore, this justifies the development of an index on which we can infer the GPD parameters of the damage function due to hazards.

From the Spring-Summer variations of this index, we determine the Generalized Pareto Distribution parameters of the daily I_{YV} index, when the (daily) values exceed the 95th quantile. As the daily values are temporally correlated (by construction, as the indice is a running sum), we consider the maxima of clusters above the 90th quantile and determine the number of days that exceed the 95th quantile threshold. This procedure is advocated in the textbook of Coles (2001).

The values and standard errors of the GPD parameters (threshold, scale and shape), and the Poisson parameters for the duration and return periods of events are shown in ~~figure ??.~~ Table 1. The values of the GPD parameters are consistent with the existing literature (e.g. Parey, 2008; Kharin et al., 2013).

We considered the range of parameters obtained from the 5 stations and their uncertainties, and took a conservative envelope of those parameters and their lower and upper uncertainties. From those ranges of parameters, we can simulate Generalized Pareto distributions for the damage function in the model of Eq. (9).

4 Experimental design

The physiological parameter in Eq. (8) are fixed to ~~$b = 0.05$, $p = 5$~~ $b = 25$, $p_0 = 25$ and $R_{\max} = 100$. We simulate $N = 10^6$ trajectories of $R(t)$ of 100 years, with an initial condition of $R(0) = 60$.

For each trajectory, the parameters of the damage function $S(t)$ are randomly sampled with a uniform distribution with a range that is estimated from the heat/drought stress indice I_{YV} (in Sec. 3). The bounds of the uniform distributions are given in table 1~~, which are conservative bounds of Figure ??.~~.

From those ensembles of simulations trajectories we determine the average of reserve $R(t)$ before ruin $\langle R \rangle$, and the time of ruin T_{ruin} (if it ever occurs). By construction of the model, $R(t)$ evolves between 0 and ~~80~~ 100 (the optimal reserve) and T_{ruin} is between 1 (immediate ruin) and 100 (no ruin within 100 year simulations).

The large number of trajectories (10^6) helps investigate the dependence of $\langle R \rangle$ and T_{ruin} on the parameters of S, namely σ, ξ, λ and Λ (see table 1).

~~Range of values of parameters for the damage function $S(t)$. The bounds are conservative values read from Figure ??.~~

~~Parameter Interpretation range u GPD threshold 1; 5 σ GPD Scale $[0.08; 0.2]$ ξ GPD shape $[-0.45; -0.2]$ λ Nb. dry days $[2; 30]$ Λ Return period of HW events (years) $[2; 15]$~~

5 Results

The dependence of the ruin time on the four damage parameters is shown in Figure 2 when $B = 0$. Each boxplot depicts the probability distribution of ruin times for a given value of a parameter, and a random combination of other parameters.

Figure 2 highlights the fact that the system can shift from a "no ruin" state to a probable ruin in a century, with rather small parameter changes of the frequency of hot days (either the frequency of dry/hot summers, or the number of dry/hot days during a hot summer). The dependence on the scale parameter σ and the shape parameter ξ is rather weak (Figure 2cd). The prescribed range of variations of those GPD parameters is small in absolute values. The GPD threshold u has an important impact of the ruin time, as the probability distribution of ruin times shift from a median on 100 years to a median value of 70 years within a 6% change of the threshold u (Figure 2e).

We define a bifurcation of ruin probability when the median ruin year τ becomes less than 100 years. From this experiment ($B = 0$), we find that a "no ruin/ruin" bifurcation occurs when a return period threshold of ~~8~~ 9 years is crossed (Figure 2a) is crossed. If we focus on the last 20 years in western Europe, extreme summer heatwaves and droughts occurred in 2003, 2006, 2018 and 2019. This might imply that European forests with trees that yield those physiological parameters are close a threshold of ~~ruin~~positive ruin probability.

The threshold on the number of hot days per summer is 14 days (Figure 2b). This parameter controls the magnitude of the random sum in $S(t)$, because the daily hazards X_k yield a bounded tail ($\xi < 0$). This means that if the length of heatwaves can exceed 14 days, tree ruin becomes significantly likely before the end of the 100 years. Such an event occurred in 2018 in Europe (Yiou et al., 2020).

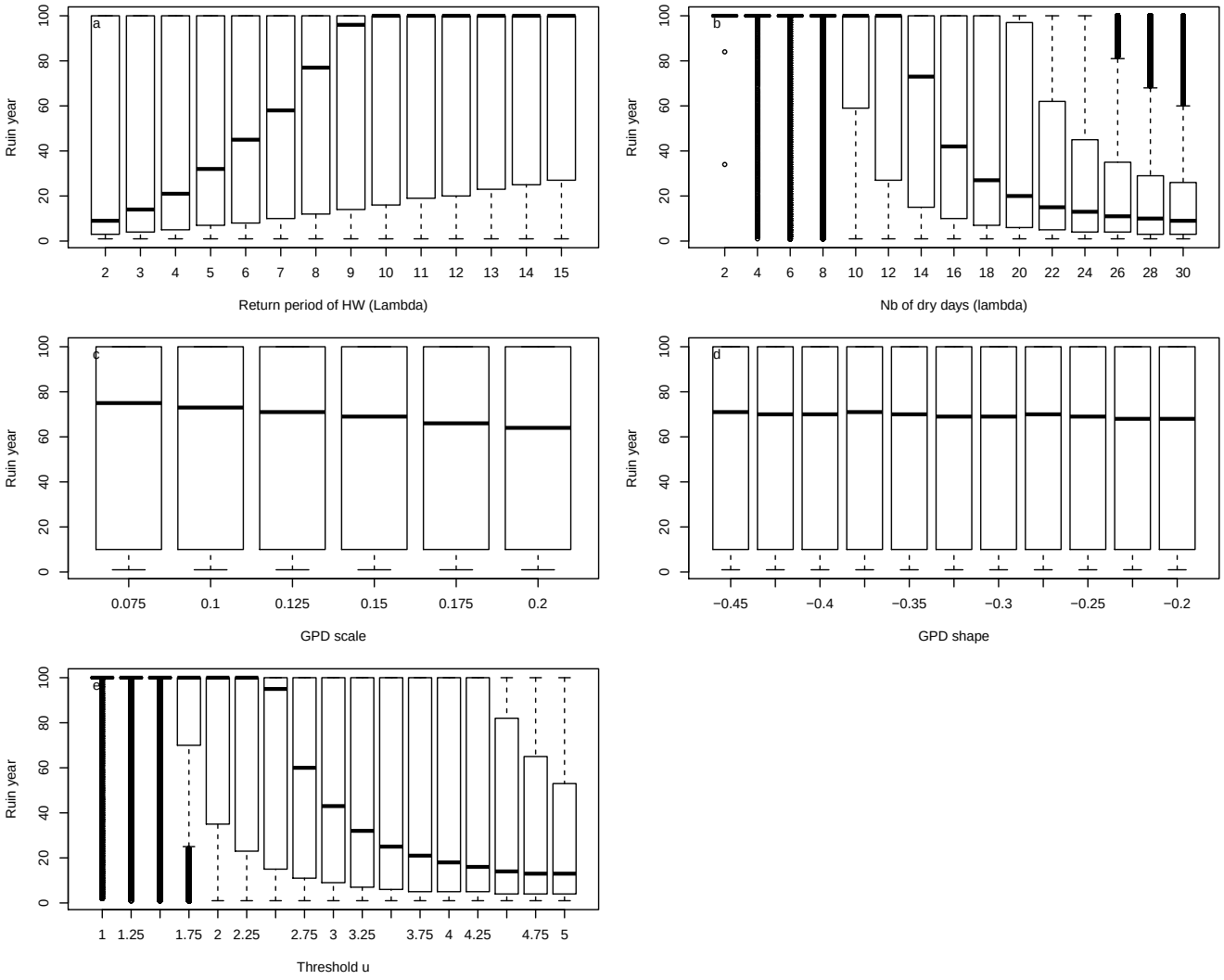

Figure 2. Dependence of probability distributions of ruin year τ as a function of drought/heatwave (HW) return periods Λ (a), number of hot days during summers λ (b), GPD fit scale μ (c) and GPD fit shape ξ (d), and threshold u above which damage $S(t)$ is triggered (e). Experiments for $B = 0$. For each value of the control variable, a boxplot is given. The horizontal thick bar of boxplots represents the median ($q50$) of the distribution. The boxes boundaries represent the 25th quantile ($q25$) and the 75th quantile ($q75$). The upper whiskers are $\min[\max(\tau), 1.5 \times (q75 - q25) + q50]$. The lower whisker has the symmetric formulation. The points are for data that are above or below the whiskers.

345 The probability distribution of the average reserve before ruin $\langle R \rangle$ is shown in Figure 3 for trees with $B = 0$. This figure highlights that $\langle R \rangle$ weakly depends on the GPD parameters of the damage function (Figure 3cd). The average reserve strongly

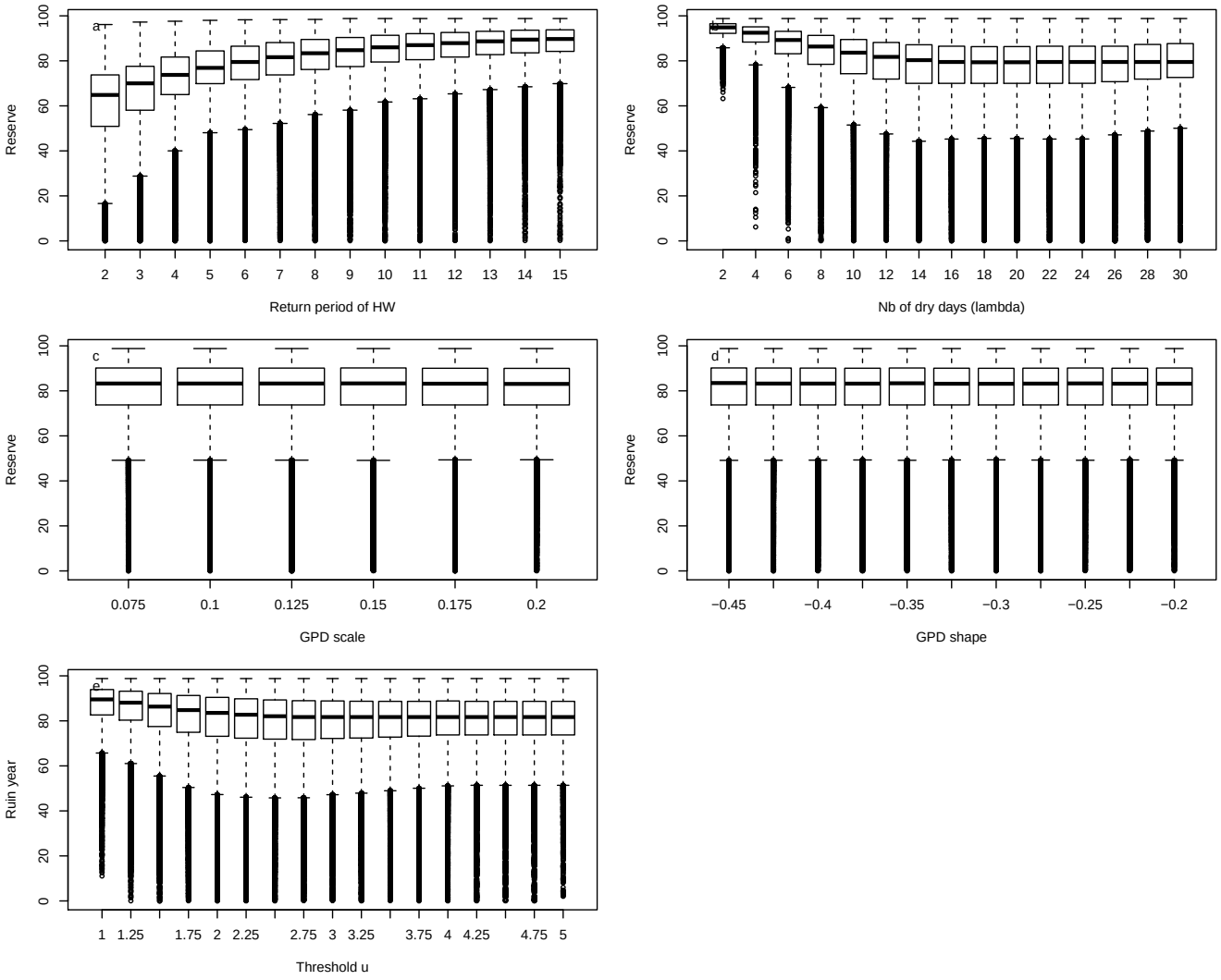

Figure 3. Dependence of probability distributions of average reserve before ruin $\langle R \rangle$ as a function of drought/heatwave (HW) return periods Λ (a), number of hot days during summers λ (b), GPD fit scale μ (c) and GPD fit shape ξ (d), and GPD threshold u (e). Experiments are for $B = 0$. For each value of the control variable, a boxplot is given. The horizontal thick bar of boxplots represents the median ($q50$) of the distribution. The boxes boundaries represent the 25th quantile ($q25$) and the 75th quantile ($q75$). The upper whiskers are $\min[\max(\langle R \rangle), 1.5 \times (q75 - q25) + q50]$. The lower whisker has the symmetric formulation.

depends on the return period of heatwaves and the number of hot days during heatwaves and the GPD threshold u (Figure 3abe).

Figure 3a shows that when damages (due to droughts/heatwaves) occur too often (low return periods of events), then the trees do not have enough time to build enough reserves to face the next extremes.

The behavior of tree growth when ~~$B = 1.5$ ("credit") is very~~ $B = 0.4$ (anisohydric) is qualitatively similar to the one with $B = 0$ (~~"cash") as the differences are relatively small (not shown): the median reserve for the "cash" simulations appear slightly higher than the "credit" simulations~~isohydric) (Figure 4). The bifurcation thresholds for Λ is 6 years, 16 days for λ, and a GPD threshold u value of 3. This suggests a higher resilience of trees with interannual memory ($B > 0$), as the bifurcations occur for higher values of Λ, λ and u.

In a second set of experiments, we maintain the scale and shape parameters constant: $\sigma = 0.1$ and $\xi = -0.3$. The other hazard parameters are randomly sampled within the range as indicated in Table 1. As observed in Figure 2ab, a transition from a median ruin time of 100 years (i.e. no or unlikely ruin) to a ruin time $\tau < 100$ years appears for return times of events Λ ~~near 8 years,~~ between 6 and 10 years, for duration of events λ ~~of 14 daysor~~ between 12 and 16 days, and for a GPD threshold u ~~of 2.75.~~ between 2.25 and 3. Therefore, we focus on the probability distributions of ruin times and reserve near those thresholds, for the ~~"cash"~~ isohydric ($B = 0$) and ~~"credit" ($B = 1.5$~~anisohydric ($B = 0.4$) simulations.

Figure 5 summarizes the probability distributions of ruin times and reserve for simulations for all simulations, and simulations ~~near $\Lambda = 8$ yearsand $\lambda = 14$ days~~with hazard values $\Lambda \in [6, 10]$ years, $\lambda \in [12, 16]$ days, and $u \in [2.25, 3]$. On the whole, the probability of ruin Ψ for $B = 0$ is ≈ 0.53, which $\Psi \approx 0.47$ for $B = 0.4$. Figure 5a shows that the ~~"credit" simulations generally~~ anisohydric simulations ($B = 0.4$) yield a larger median value of ruin time (~~between 3 and 8 years~~ 100 years vs 74 years for $B = 0$). This means that ~~a "credit"~~ an anisohydric strategy leads to a ~~slightly~~ longer life expectancy. The differences in the reserve ~~are hard to see from~~ shown in Figure 5b~~, although significant with a~~ . A Kolmogorov-Smirnov test (von Storch and Zwiers, 2001) ~~.~~ indicates a significantly higher value of average reserve for $B = 0$ (83 vs. 81, p-value $< 10^{-15}$). The differences amount to ≈ 2 units of reserve, which is small compared to the optimal value ~~. We note that "cash" ($B = 0$) simulations have a higher median reserve than the "credit" simulations for the whole ensemble or near $\Lambda = 8$ years. However, the "credit" simulations ($B = 1.5$) do have a higher median for $\lambda = 14$ days and threshold $u = 2.75$.~~ $R_{\max} = 100$.

~~Globally~~On the whole, those results show the dependence of the ruin time on the coping strategy: smoothing the damages over two years increases the ruin time, for various scenarios of extremes (return time, length and intensity). However, the response of the reserve depends on the parameter of extreme: a higher frequency (or lower return period Λ) favors ~~"cash"~~ isohydric strategies, while the intensity (linked to the duration or highest value) slightly favors ~~"credit"~~ anisohydric strategies. Therefore, there is no binary response of this type of model to the hazard parameters, and this emphasizes the potential nonlinearity of tree response (Flach et al., 2018).

6 Conclusions

This paper presents a paradigm based on ruin theory to investigate tipping points ~~or collapse~~ to a ruin of trees by estimating the chance that systems which are subject to extreme events are damaged to the point of ~~disappearing. It provides a quantification (and uncertainties) to the question of vulnerability of ecosystems with long expected life~~dying. We described the vulnerability of an idealized forest by its probability of dying through the loss of growing ability, and illustrated a statistical methodology to identify climate parameters that control ruin time. This proof of concept was applied to tree growth, but it could be extended

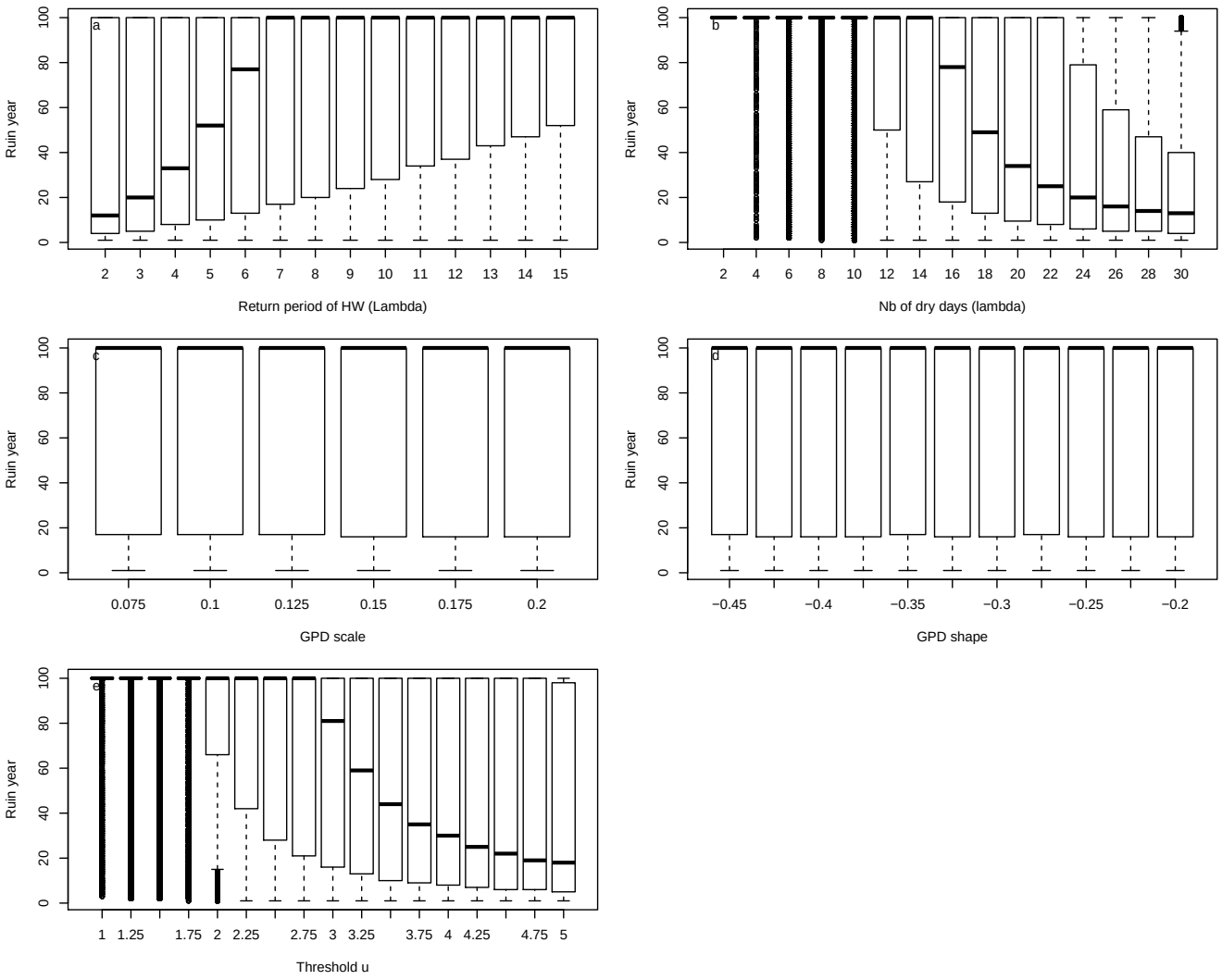

Figure 4. Dependence of probability distributions of ruin year τ as a function of drought/heatwave (HW) return periods Λ (a), number of hot days during summers λ (b), GPD fit scale μ (c) and GPD fit shape ξ (d), and threshold u above which damage $S(t)$ is triggered (e). Experiments for $B = 0.4$. For each value of the control variable, a boxplot is given. The horizontal thick bar of boxplots represents the median ($q50$) of the distribution. The boxes boundaries represent the 25th quantile ($q25$) and the 75th quantile ($q75$). The upper whiskers are $\min[\max(\tau), 1.5 \times (q75 - q25) + q50]$. The lower whisker has the symmetric formulation. The points are for data that are above or below the whiskers.

to all types of eco-systems that are vulnerable to climate hazards ~~. This paradigm presents natural and operational features to estimate risks under climate change. It explicitly combines hazards, exposure and "fragility" to determine risks.~~ on long time

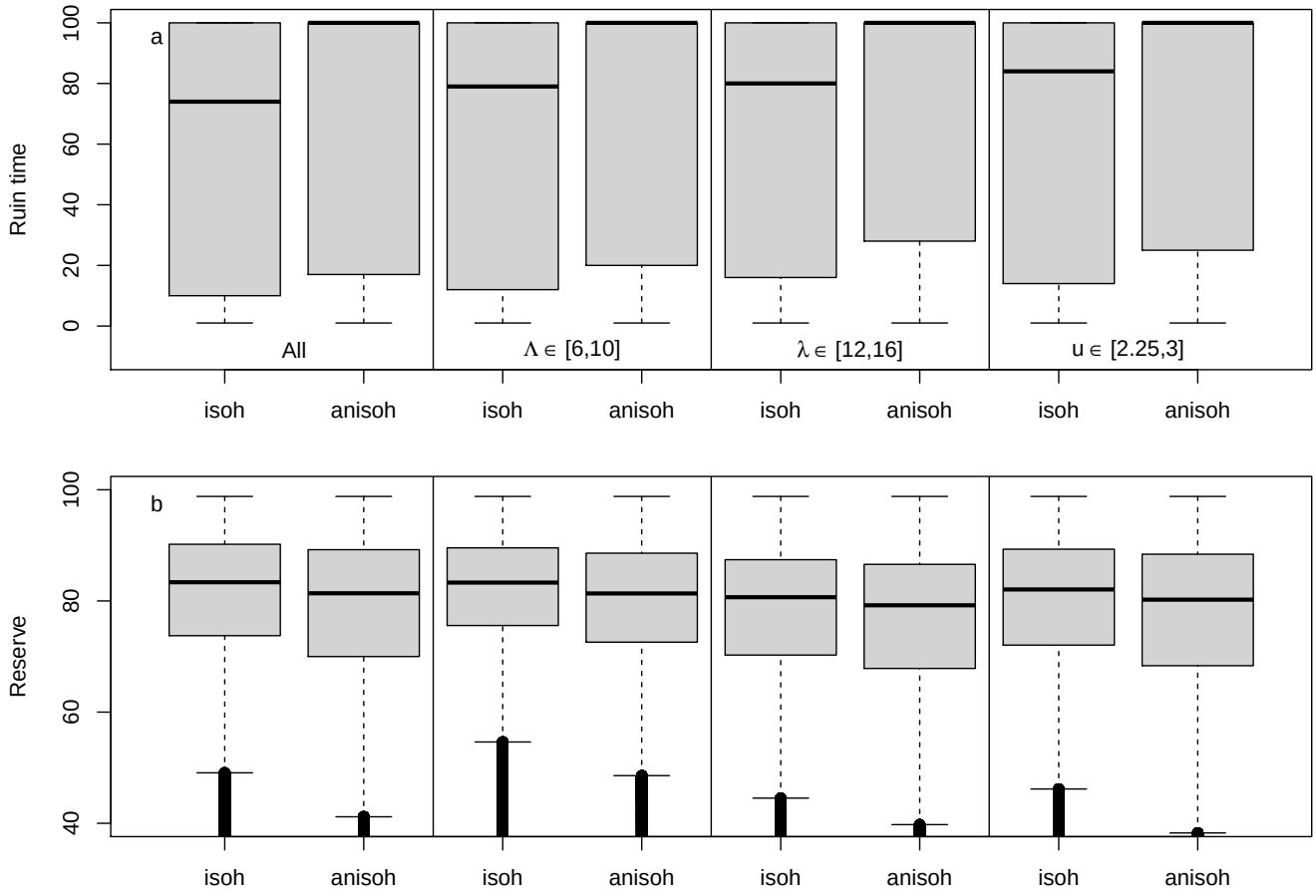

Figure 5. Conditional probability distribution of ruin times (panel a) and reserve (panel b). The first two boxplots (~~"cash"~~ isohydric ($B = 0$) and ~~"credit"~~anisohydric ($B = 0.4$)) are for all simulations. The ~~"cashRT" and "creditT"~~ second boxplots are for return periods Λ of droughts/heatwaves of ~~8~~ 6–10 years for ~~"cash"~~ isohydric and ~~"credit"~~ anisohydric simulations. The ~~"cashNb" and "credit1Nb"~~ third boxplots are for ~~14~~ durations λ of 12–16 days of drought/heatwave in a summer. The ~~"cashu" and "creditu"~~ last boxplots are for ~~a fixed threshold $u = 2.75$~~GPD thresholds of 2.25–3.

scales. A careful determination of the physiological parameters of the model, from in situ observations, is necessary for an operational application. Such a task would be a project in itself.

The example we took ~~permits~~ helps to make decisions on forestry from a priori information on climate change. The model we treated only accounts for one type of natural hazard. Others (including storms or fires) could be included, although the recovery rate (or "strategy") must be adapted to each type of hazard.

We have investigated how variations of the hazard ~~parameter~~ parameters affect the damage function and the probability of ruin. It appears that the most critical parameters are linked to the frequency of extreme events and average intensity, which affect the rate of recovery of the trees.

We have examined the impact of "strategies" to cope with extremes. Although small, this impact has a differential effect on the average tree reserve and the probability of ruin: with this model, trees that have an average lower probability of ruin also have a lower average reserve, if the hazard frequency changes (Figure 5). If the hazard average intensity changes (longer or more intense), then trees with a lower probability of ruin also have a (slightly) higher reserve.

This subtlety shows the richness of this model, and emphasizes the need to have a proper definition of the hazard (Cattiaux and Ribes, 2018) and how hazards change with time, which is the topic of extreme event attribution (National Academies of Sciences Engineering and Medicine, 2016).

This study has obvious caveats. The growth/ruin model is exceedingly simple and does not reflect real trees, as the Cramer-Lundberg does not reflect the complexity of the insurance sector. The proposed tree model is mainly a proof or concept, which could be enriched with other bio-physical ingredients. Nevertheless, a key point is that however complex, a ruin model should be simplifiable to a Cramer-Lundberg model.

Many mathematical papers have described the exact properties of the Cramer-Lundberg model (e.g Embrechts et al., 1997, for a review). Our tree ruin/growth model violates some of the simple assumptions of the basic Cramer-Lundberg model, namely the time independence of $R(t)$ in the ~~"credit"~~ anisohydric mode. This forbids explicit formulas of ruin times. This is why we resort to extensive numerical Monte Carlo simulations. Those simulations ($\approx 10^6$ trajectories of 100 years) take less than 4 mn on a 12 core computer, which helps circumventing this mathematical shortcoming.

The drought/heat stress indice we constructed is also rather crude and could be refined, although it was only designed to determine parameters of a Pareto distribution, and we did not use it anymore in the study because we simulate random laws (Pareto and Poisson) with parameters that are ~~experimentally~~ numerically determined from the indice. All simulations were performed in a stationary mode, albeit with random selections of parameters. Nonstationary simulations could be envisaged to explicitly take climate change into account. Data from climate model simulations could hence be used to simulate hazards ~~(e.g. Herrera-Estrada and Sheffield, 2017)~~(e.g. Herrera-Estrada and Sheffield, 2017; Massey et al., 2015). This is left to future studies.

Some of the parameters (especially the impact scaling) we used were chosen heuristically. Finer in situ studies and expertise would be necessary to tune those parameters to each tree species.

Code and data availability. The simulation code and sample data to produce the drought index are available from https://zenodo.org/badge/DOI/10.5281/zenodo.4075163.svg

Appendix A: Drought/heatwave index definition

As this paper is more a proof-of-concept for a ruin model than a detailed study (which will be performed later), we consider simplified drought/heat hazard index that can easily be computed from climatological observations. We are interested in an index that reflects a compound event (Zscheischler et al., 2020) with extended dry period and high temperatures. There are a few indices of drought or aridity that consider precipitation and temperature (Baltas, 2007). The index of De Martonne (1926) normalizes cumulated precipitation and average temperature:

$$I_{DM} = \frac{P}{T+10}, \tag{A1}$$

where the numerator is the cumulated precipitation and T is the mean temperature (in Celsius). This index was used to determine drought zones. Time variations of this index can be obtained by considering only yearly or seasonal averages of precipitation and temperature. The $+10$ term in the denominator of Eq. (A1) is ad hoc to scale the respective variations of precipitation and temperature. Droughts are obtained with small values of this index (low precipitation and high temperature values).

Although easy to compute, this simple index yields a few drawbacks. The main one is that it mainly reflects wetness, not drought. Most of of its variability is connected with the variability of precipitation and the upper tail of its probability distribution. Therefore seasons with little rain produce little variability in the index. One way to circumvent this would be to invert the index (i.e. consider $1/I_{DM}$). This is still not very satisfactory because the value of I_{DM} for summers with notoriously dry heatwaves (e.g., 1976 and 2003) in Europe are just within the average and do not show anything special, contrary to what is expected (Ciais et al., 2005).

Thus, we propose an alternative drought index, still based on daily precipitation and temperature. For a given day j, we consider D_j the frequency of precipitation: $D_j = 0$ if precipitation $P_j > 0.5$ mm/day, $D_j = 1$ if $P_j \leq 0.5$mm/day. We then construct an aridity index based on the weighted drought frequency and temperature.

$$I_{\mathrm{YV}}(t) = \sum_{j=t-30}^{t} T_j \times (D_j + a) A \exp(-(t-j)/30) \tag{A2}$$

where t is time (in days), $a \geq 0$ is a scaling constant (similar to $+10$ in Eq. (A1)) and T_j is maximum daily temperature (TX in ECA&D (Klein-Tank et al., 2002)). $A \approx 30$ is a scaling constant to ensure that the sum of exponential weights is 1. In this paper, we chose $a = 1$ after a few tuning tests to verify that the index yields high values during notoriously dry years (e.g., 1976, 2003 or 2018).

This daily index is analogous to the inverse of the De Martonne index. One refinement comes from the exponential weights that give more importance to recent days than remote days. We can then compute the monthly median, upper quantiles and maximum of I_{YV}. We compute this index by starting on March 1st, as it is generally when the tree phenology resumes after the winter season, in the Northern midlatitudes. The daily index is computed until September 30th, when the vegetative cycle is almost finished.

With this new drought index, the extreme drought/heatwaves of 1976 and 2003 do become exceptional, as expected from the literature (Ciais et al., 2005). Figure A1 compares the precipitation, temperature, de Martonne index and the new I_{YV} index for temperature and precipitation observations in Orly (near Paris, France). The precipitation or number of dry days do not yield extreme values for years with notorious heat stress in France (e.g. 1976, 2003 or 2019), as they are close to the 25–75th quantile values (Figure A1bd). Therefore, the De Martonne aridity indice does not yield particularly extreme values for those years (Figure A1c).

To better evaluate how the new index defined was a pertinent indicator for impact of climate on vegetation stress, we used the ORCHIDEE land surface model (Krinner et al., 2005) to simulate both the soil moisture and tree net primary production (NPP). We made a simulation using the ERA5 land atmospheric reanalyses at $0.1°\times0.1°$ resolution (Hersbach et al., 2020) for the gridcell including Orly between 1981 and 2019. Atfer a spin-up of 200 years using the first 10 year of the forcing, the simulation was done for the entire period. The variations of soil moisture serve as input for the hazard function and are a refinement over precipitation only. As an indicator of vegetation damage, we consider the number of days for which NPP is below the 10th quantile (0.15 gC/day/m^2), which indicates a "risk zone" for trees (Fig. A1f).

We find a significant (negative) correlation between the percentage of dry days and relative humidity for the 1981–2019 period (Fig. A1c), with $r = -0.7$ and p-value $< 10^{-6}$. The NPP variation are significantly (anti) correlated with the I_{YV} index ($r = -0.7$, p-value $< 10^{-6}$). The percentage of days for which NPP is below the 10th quantile corresponds to the exceedances of the I_{YV} index above a high threshold (Fig. A1e). Therefore, we believe that the choice of this index carries a physical meaning and can be used as a proxy to compute the parameters of a damage function.

We computed this I_{YV} indice on five stations from ECA&D (Klein-Tank et al., 2002): Berlin, Orly, Toulouse, De Bilt and Madrid. Those five stations cover a large part western Europe.

Author contributions. PY and NV co-constructed the growth model. PY designed the ruin model simulations. NV computed the relative humidity and NPP indices for validation. PY made the figures. Both authors contributed to the text.

Competing interests. The authors declare no competing interest.

Disclaimer. TEXT

Acknowledgements. This work was supported by an ERC grant No. 338965-A2C2 and a French ANR grant (SAMPRACE).

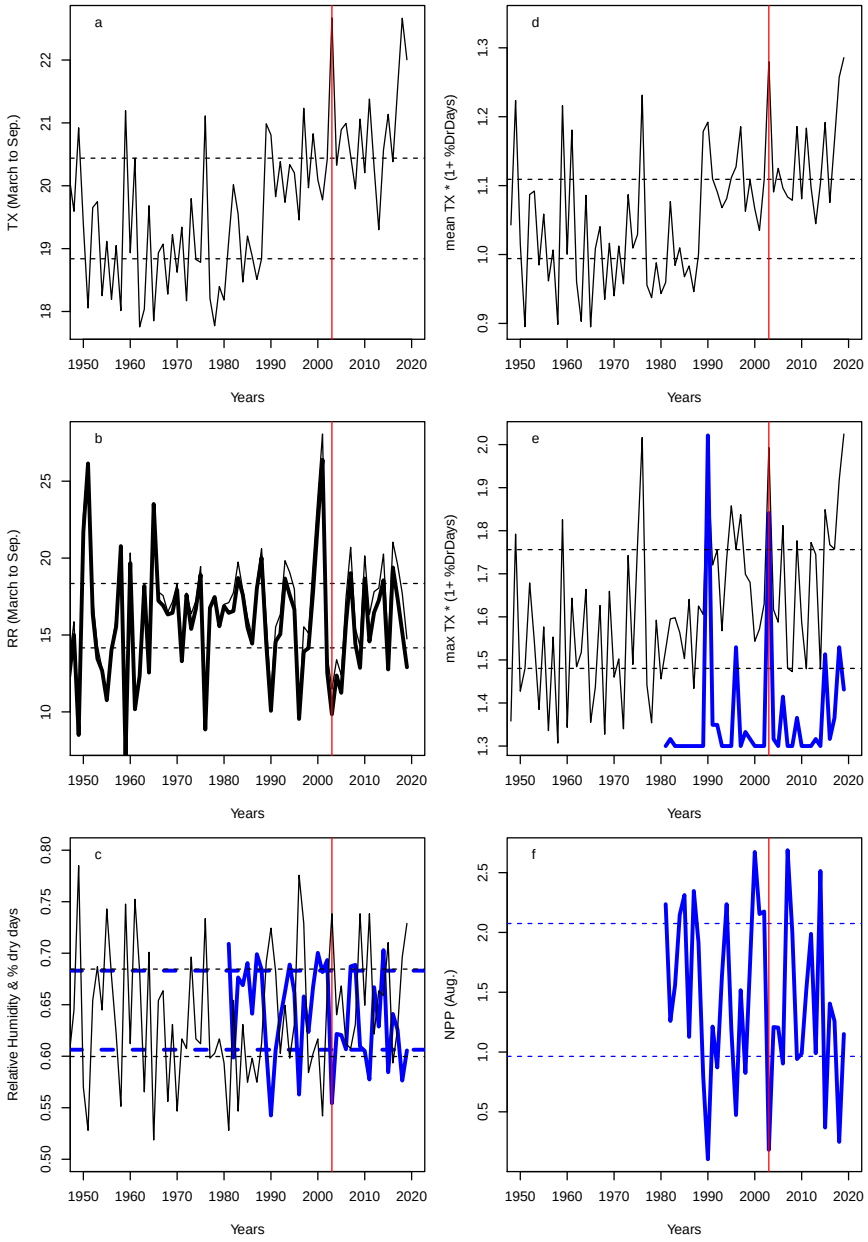

Figure A1. Variations of indices for Orly. Horizontal dashed lines for $q25$ and $q75$ quantiles. The vertical red lines are indicate 2003. a: Average (March to September) temperature in Orly. b: Average (March to September) precipitation in Orly (thin line); scaled De Martonne index (by 28) (thick black line). c: percentage of dry days between March and September (black line) and relative humidity (thick blue line). d: March to September mean of I_{YV} index. e: Daily maximum of I_{YV} index (black line) and scaled number of days when NPP is below the 10th quantile (thick blue line). f: NPP variations in Orly from an ORCHIDEE model simulation forced by the ERA5 reanalysis.

References

Adams, H. D., Guardiola-Claramonte, M., Barron-Gafford, G. A., Villegas, J. C., Breshears, D. D., Zou, C. B., Troch, P. A., and Huxman, T. E.: Temperature sensitivity of drought-induced tree mortality portends increased regional die-off under global-change-type drought, Proceedings of the national academy of sciences, 106, 7063–7066, iSBN: 0027-8424 Publisher: National Acad Sciences, 2009.

Allen, C. D., Macalady, A. K., Chenchouni, H., Bachelet, D., McDowell, N., Vennetier, M., Kitzberger, T., Rigling, A., Breshears, D. D., and Hogg, E. T.: A global overview of drought and heat-induced tree mortality reveals emerging climate change risks for forests, Forest ecology and management, 259, 660–684, 2010.

Anderegg, W. R., Kane, J. M., and Anderegg, L. D.: Consequences of widespread tree mortality triggered by drought and temperature stress, Nature climate change, 3, 30–36, iSBN: 1758-6798 Publisher: Nature Publishing Group, 2013.

Anderegg, W. R., Flint, A., Huang, C.-y., Flint, L., Berry, J. A., Davis, F. W., Sperry, J. S., and Field, C. B.: Tree mortality predicted from drought-induced vascular damage, Nature Geoscience, 8, 367–371, iSBN: 1752-0908 Publisher: Nature Publishing Group, 2015a.

Anderegg, W. R., Schwalm, C., Biondi, F., Camarero, J. J., Koch, G., Litvak, M., Ogle, K., Shaw, J. D., Shevliakova, E., and Williams, A. P.: Pervasive drought legacies in forest ecosystems and their implications for carbon cycle models, Science, 349, 528–532, iSBN: 0036-8075 Publisher: American Association for the Advancement of Science, 2015b.

Asmussen, S. and Albrecher, H.: Ruin probabilities, World Scientific Publishing Co Pte Ltd, 2010.

Baltas, E.: Spatial distribution of climatic indices in northern Greece, Meteorological Applications: A journal of forecasting, practical applications, training techniques and modelling, 14, 69–78, iSBN: 1350-4827 Publisher: Wiley Online Library, 2007.

Barbaroux, C., Bréda, N., and Dufrêne, E.: Distribution of above-ground and below-ground carbohydrate reserves in adult trees of two contrasting broad-leaved species (Quercus petraea and Fagus sylvatica), New Phytologist, 157, 605–615, iSBN: 1469-8137 Publisher: Wiley Online Library, 2003.

Bastos, A., Ciais, P., Friedlingstein, P., Sitch, S., Pongratz, J., Fan, L., Wigneron, J. P., Weber, U., Reichstein, M., Fu, Z., Anthoni, P., Arneth, A., Haverd, V., Jain, A. K., Joetzjer, E., Knauer, J., Lienert, S., Loughran, T., McGuire, P. C., Tian, H., Viovy, N., and Zaehle, S.: Direct and seasonal legacy effects of the 2018 heat wave and drought on European ecosystem productivity, Science Advances, 6, eaba2724, https://advances.sciencemag.org/content/advances/6/24/eaba2724.full.pdf, type: 10.1126/sciadv.aba2724, 2020.

Bigler, C., Gavin, D. G., Gunning, C., and Veblen, T. T.: Drought induces lagged tree mortality in a subalpine forest in the Rocky Mountains, Oikos, 116, 1983–1994, iSBN: 0030-1299 Publisher: Wiley Online Library, 2007.

Bréda, N. and Badeau, V.: Forest tree responses to extreme drought and some biotic events: towards a selection according to hazard tolerance?, Comptes Rendus Geoscience, 340, 651–662, iSBN: 1631-0713 Publisher: Elsevier, 2008.

Cailleret, M., Jansen, S., Robert, E. M., Desoto, L., Aakala, T., Antos, J. A., Beikircher, B., Bigler, C., Bugmann, H., and Caccianiga, M.: A synthesis of radial growth patterns preceding tree mortality, Global change biology, 23, 1675–1690, iSBN: 1354-1013 Publisher: Wiley Online Library, 2017.

Cattiaux, J. and Ribes, A.: Defining single extreme weather events in a climate perspective, Bulletin of the American Meteorological Society, https://doi.org/https://doi.org/10.1175/BAMS-D-17-0281.1, 2018.

Choat, B., Jansen, S., Brodribb, T. J., Cochard, H., Delzon, S., Bhaskar, R., Bucci, S. J., Feild, T. S., Gleason, S. M., and Hacke, U. G.: Global convergence in the vulnerability of forests to drought, Nature, 491, 752, 2012.

Ciais, P., Reichstein, M., Viovy, N., Granier, A., Ogee, J., Allard, V., Aubinet, M., Buchmann, N., Bernhofer, C., Carrara, A., Chevallier, F., De Noblet, N., Friend, A., Friedlingstein, P., Grunwald, T., Heinesch, B., Keronen, P., Knohl, A., Krinner, G., Loustau, D., Manca, G.,

Matteucci, G., Miglietta, F., Ourcival, J., Papale, D., Pilegaard, K., Rambal, S., Seufert, G., Soussana, J., Sanz, M., Schulze, E., Vesala, T., and Valentini, R.: Europe-wide reduction in primary productivity caused by the heat and drought in 2003, Nature, 437, 529–533, <GotoISI>://000232004800045, 2005.

Coles, S.: An introduction to statistical modeling of extreme values, Springer series in statistics, Springer, London, New York, 2001.

De Martonne, E.: A new climatological function: The Aridity Index, Gauthier-Villars, Paris, France, 1926.

DeSoto, L., Cailleret, M., Sterck, F., Jansen, S., Kramer, K., Robert, E. M., Aakala, T., Amoroso, M. M., Bigler, C., and Camarero, J. J.: Low growth resilience to drought is related to future mortality risk in trees, Nature communications, 11, 1–9, iSBN: 2041-1723 Publisher: Nature Publishing Group, 2020.

Diamond, J.: Collapse: How societies choose to succeed or fail, Viking Penguin: New York, 2005.

Embrechts, P., Klüppelberg, Claudia, C., and Mikosch, T.: Modelling extremal events for insurance and finance, vol. 33 of *Applications of mathematics*, Springer, Berlin ; New York, 1997.

Feller, W.: An Introduction to Probability Theory and Its Applications, vol. I, J. Wiley & Sons, New York, London, Sydney, 3rd edition edn., 1950.

Field, C. B., Barros, V., Stocker, T. F., and Dahe, Q.: Managing the risks of extreme events and disasters to advance climate change adaptation: special report of the intergovernmental panel on climate change, Cambridge University Press, 2012.

Flach, M., Sippel, S., Gans, F., Bastos, A., Brenning, A., Reichstein, M., and Mahecha, M. D.: Contrasting biosphere responses to hydrometeorological extremes: revisiting the 2010 western Russian heatwave, Biogeosciences, 16, 6067–6085, 2018.

Han, J. and Singh, V. P.: Forecasting of droughts and tree mortality under global warming: a review of causative mechanisms and modeling methods, Journal of Water and Climate Change, 2020.

Haylock, M. R., Hofstra, N., Tank, A. M. G. K., Klok, E. J., Jones, P. D., and New, M.: A European daily high-resolution gridded data set of surface temperature and precipitation for 1950-2006, J. Geophys. Res. - Atmospheres, 113, doi:10.1029/2008JD010 201, <GotoISI>: //000260598000009, 2008.

He, W., Liu, H., Qi, Y., Liu, F., and Zhu, X.: Patterns in nonstructural carbohydrate contents at the tree organ level in response to drought duration, Global change biology, 26, 3627–3638, iSBN: 1354-1013 Publisher: Wiley Online Library, 2020.

Herrera-Estrada, J. E. and Sheffield, J.: Uncertainties in future projections of summer droughts and heat waves over the contiguous United States, Journal of Climate, 30, 6225–6246, iSBN: 0894-8755, 2017.

Hersbach, H., Bell, B., Berrisford, P., Hirahara, S., Horányi, A., Muñoz-Sabater, J., Nicolas, J., Peubey, C., Radu, R., and Schepers, D.: The ERA5 global reanalysis, Quat. J. Roy. Met. Soc., 146, 1999–2049, iSBN: 0035-9009 Publisher: Wiley Online Library, 2020.

Katz, R. W.: Weather and climate disasters, Extreme Value Modeling and Risk Analysis: Methods and Applications, 21, 439–60, 2016.

Kharin, V. V., Zwiers, F. W., Zhang, X., and Wehner, M.: Changes in temperature and precipitation extremes in the CMIP5 ensemble, Climatic change, 119, 345–357, iSBN: 0165-0009 Publisher: Springer, 2013.

Klein-Tank, A., Wijngaard, J., Konnen, G., Bohm, R., Demaree, G., Gocheva, A., Mileta, M., Pashiardis, S., Hejkrlik, L., Kern-Hansen, C., Heino, R., Bessemoulin, P., Muller-Westermeier, G., Tzanakou, M., Szalai, S., Palsdottir, T., Fitzgerald, D., Rubin, S., Capaldo, M., Maugeri, M., Leitass, A., Bukantis, A., Aberfeld, R., Van Engelen, A., Forland, E., Mietus, M., Coelho, F., Mares, C., Razuvaev, V., Nieplova, E., Cegnar, T., Lopez, J., Dahlstrom, B., Moberg, A., Kirchhofer, W., Ceylan, A., Pachaliuk, O., Alexander, L., and Petrovic, P.: Daily dataset of 20th-century surface air temperature and precipitation series for the European Climate Assessment, Int. J. Climatol., 22, 1441–1453, 2002.

Krinner, G., Viovy, N., de Noblet-Ducoudré, N., Ogée, J., Polcher, J., Friedlingstein, P., Ciais, P., Sitch, S., and Prentice, I. C.: A dynamic global vegetation model for studies of the coupled atmosphere-biosphere system, Global Biogeochemical Cycles, 19, https://doi.org/10.1029/2003GB002199, iSBN: 0886-6236 Publisher: Wiley Online Library, 2005.

Lenton, T. M., Held, H., Kriegler, E., Hall, J. W., Lucht, W., Rahmstorf, S., and Schellnhuber, H. J.: Tipping elements in the Earth's climate system, Proc. Natl. Acad. Sci. USA, 105, 1786–1793, https://doi.org/DOI 10.1073/pnas.0705414105, <GotoISI>://000253261900005, 2008.

Levermann, A., Bamber, J. L., Drijfhout, S., Ganopolski, A., Haeberli, W., Harris, N. R. P., Huss, M., Kruger, K., Lenton, T. M., Lindsay, R. W., Notz, D., Wadhams, P., and Weber, S.: Potential climatic transitions with profound impact on Europe Review of the current state of six 'tipping elements of the climate system', Climatic Change, 110, 845–878, https://doi.org/DOI 10.1007/s10584-011-0126-5, <GotoISI>://000299346900019, 2012.

Lindenmayer, D., Messier, C., and Sato, C.: Avoiding ecosystem collapse in managed forest ecosystems, Frontiers in Ecology and the Environment, 14, 561–568, iSBN: 1540-9295 Publisher: Wiley Online Library, 2016.

Lundberg, F.: Approximerad framstallning af sannolikhetsfunktionen: Aterforsakring af kollektivrisker, Almqvist & Wiksell, 1903.

Massey, N., Jones, R., Otto, F. E. L., Aina, T., Wilson, S., Murphy, J. M., Hassell, D., Yamazaki, Y. H., and Allen, M. R.: weather@home—development and validation of a very large ensemble modelling system for probabilistic event attribution, Quat. J. Roy. Met. Soc., 141, 1528–1545, https://doi.org/10.1002/qj.2455, 2015.

Matusick, G., Ruthrof, K. X., Kala, J., Brouwers, N. C., Breshears, D. D., and Hardy, G. E. S. J.: Chronic historical drought legacy exacerbates tree mortality and crown dieback during acute heatwave-compounded drought, Environmental Research Letters, 13, 095 002, iSBN: 1748-9326 Publisher: IOP Publishing, 2018.

Mitchell, P. J., O'Grady, A. P., Tissue, D. T., White, D. A., Ottenschlaeger, M. L., and Pinkard, E. A.: Drought response strategies define the relative contributions of hydraulic dysfunction and carbohydrate depletion during tree mortality, New Phytologist, 197, 862–872, iSBN: 0028-646X Publisher: Wiley Online Library, 2013.

National Academies of Sciences Engineering and Medicine, ed.: Attribution of Extreme Weather Events in the Context of Climate Change, The National Academies Press, Washington, DC, https://doi.org/10.17226/21852, www.nap.edu/catalog/21852/attribution-of-extreme-weather-events-in-the-context-of-climate-change, 2016.

Parey, S.: Extremely high temperatures in France at the end of the century, Climate Dynamics, 30, 99–112, https://doi.org/DOI 10.1007/s00382-007-0275-4, <GotoISI>://000251009500006, 2008.

Pereira, J. C. and Viola, E.: Catastrophic climate change and forest tipping points: Blind spots in international politics and policy, Global Policy, 9, 513–524, iSBN: 1758-5880 Publisher: Wiley Online Library, 2018.

Rao, K., Anderegg, W. R., Sala, A., Martínez-Vilalta, J., and Konings, A. G.: Satellite-based vegetation optical depth as an indicator of drought-driven tree mortality, Remote Sensing of Environment, 227, 125–136, iSBN: 0034-4257 Publisher: Elsevier, 2019.

Reyer, C. P., Rammig, A., Brouwers, N., and Langerwisch, F.: Forest resilience, tipping points and global change processes, Wiley Online Library, 2015.

Sippel, S., Reichstein, M., Ma, X., Mahecha, M. D., Lange, H., Flach, M., and Frank, D.: Drought, heat, and the carbon cycle: A review, Current Climate Change Reports, 4, 266–286, 2018.

Smith, R. L. and Shively, T. S.: Point process approach to modeling trends in tropospheric ozone based on exceedances of a high threshold, Atmospheric Environment, 29, 3489–3499, iSBN: 1352-2310 Publisher: Elsevier, 1995.

Teuling, A. J., Seneviratne, S. I., Stöckli, R., Reichstein, M., Moors, E., Ciais, P., Luyssaert, S., Van Den Hurk, B., Ammann, C., and Bernhofer, C.: Contrasting response of European forest and grassland energy exchange to heatwaves, Nature Geoscience, 3, 722–727, iSBN: 1752-0908 Publisher: Nature Publishing Group, 2010.

van der Molen, M. K., Dolman, A. J., Ciais, P., Eglin, T., Gobron, N., Law, B. E., Meir, P., Peters, W., Phillips, O. L., and Reichstein, M.: Drought and ecosystem carbon cycling, Agricultural and Forest Meteorology, 151, 765–773, iSBN: 0168-1923 Publisher: Elsevier, 2011.

Villalba, R. and Veblen, T. T.: Influences of large-scale climatic variability on episodic tree mortality in northern Patagonia, Ecology, 79, 2624–2640, iSBN: 1939-9170 Publisher: Wiley Online Library, 1998.

Villalba, R., Cook, E., Jacoby, G., D'Arrigo, R., Veblen, T., and Jones, P.: Tree-ring based reconstructions of northern Patagonia precipitation since AD 1600, HOLOCENE, 8, 659–674, <GotoISI>://000077236500002, 1998.

von Buttlar, J., Zscheischler, J., Rammig, A., Sippel, S., Reichstein, M., Knohl, A., Jung, M., Menzer, O., Arain, M. A., and Buchmann, N.: Impacts of droughts and extreme temperature events on gross primary production and ecosystem respiration: A systematic assessment across ecosystems and climate zones, Biogeosciences Discussions, iSBN: 1810-6277 Publisher: Copernicus, 2017.

von Storch, H. and Zwiers, F. W.: Statistical Analysis in Climate Research, Cambridge University Press, Cambridge, 2001.

Wigneron, J.-P., Fan, L., Ciais, P., Bastos, A., Brandt, M., Chave, J., Saatchi, S., Baccini, A., and Fensholt, R.: Tropical forests did not recover from the strong 2015–2016 El Niño event, Science advances, 6, eaay4603, iSBN: 2375-2548 Publisher: American Association for the Advancement of Science, 2020.

Yiou, P., Cattiaux, J., Faranda, D., Kadygrov, N., Jézéquel, A., Naveau, P., Ribes, A., Robin, Y., Thao, S., and van Oldenborgh, G. J.: Analyses of the Northern European summer heatwave of 2018, Bulletin of the American Meteorological Society, 101, S35–S40, 2020.

Zeppel, M. J., Adams, H. D., and Anderegg, W. R.: Mechanistic causes of tree drought mortality: recent results, unresolved questions and future research needs, The New Phytologist, 192, 800–803, iSBN: 0028-646X Publisher: JSTOR, 2011.

Zscheischler, J., Martius, O., Westra, S., Bevacqua, E., Raymond, C., Horton, R. M., van den Hurk, B., AghaKouchak, A., Jézéquel, A., and Mahecha, M. D.: A typology of compound weather and climate events, Nature reviews earth & environment, pp. 1–15, iSBN: 2662-138X Publisher: Nature Publishing Group, 2020.